Electronic Supplementary Material (ESI) for Journal of Materials Chemistry C.

Anion Induced Ferroelectric Polarization in a Luminescent Metal-organic Cage Compound †

Ashok Yadav,[a] Anant Kumar Srivastava,[a] Priyangi Kulkarni,[c] Pillutla Divya,[c] Alexander Steiner,[d], B. Praveenkumar*,[c] and Ramamoorthy Boomishankar*,[a,b]*

[a]Department of Chemistry, Indian Institute of Science Education and Research (IISER) Pune, Dr. Homi Bhabha Road, Pune, India - 411008, India.
*[b]Centre for Energy Science, Indian Institute of Science Education and Research (IISER), Pune, Dr. Homi Bhabha Road, Pune – 411008, India. Fax: +912025908186; *E-mail: boomi@iiserpune.ac.in*
[c]Armament Research and Development Establishment (ARDE), Defence Research and Development Organisation (DRDO), Dr. Homi Bhabha Road, Pune, India – 411008
[d]Department of Chemistry, University of Liverpool, Crown Street, Liverpool – L69 7ZD

Supporting Information

Experimental Section

General Remarks

All manipulations involving phosphorus halides were performed under a dry nitrogen atmosphere in standard Schlenk-glassware. Solvents were dried over sodium (toluene). 3-aminopyridyl was purchased from Aldrich and used as received. $PSCl_3$ was purchased locally and was distilled prior to use. The ligand TPTA was synthesized by following our earlier reported procedure.[1] NMR spectra were recorded on a Bruker 400 MHz spectrometer (^1H NMR: 400.13 MHz, $^{13}C\{^1H\}$NMR: 100.62 MHz, $^{31}P\{^1H\}$ NMR: 161.97 MHz) or on a Bruker 500 MHz (^1H NMR: 500.00 MHz, $^{13}C\{^1H\}$NMR: 125.725 MHz, $^{31}P\{^1H\}$ NMR: 202.404 MHz) spectrometer at room temperature using $SiMe_4$ (^1H, ^{13}C) and 85% H_3PO_4 (^{31}P). The mass spectra were obtained on an Applied Biosystem MALDI-TOF/TOF spectrometer. The solid-state (CP-MAS) $^{31}P\{1\ H\}$ NMR spectra were obtained on a Bruker 500 MHz spectrometer at a MAS rate of 10.0 KHz. The powder X-ray diffraction data were obtained from a Bruker D8 Advance diffractometer. Thermal analysis data has been obtained from a Perkin-Elmer STA-6000 thermogravimetric analyzer. FT-IR spectra were taken on a Perkin-Elmer spectrophotometer with samples prepared as KBr pellets. Elemental analyses were performed on a Vario-EL cube elemental analyser. Melting points were obtained using an Electrothermal melting point apparatus and were uncorrected. The absorption and emission studies were done by a Perkin-Elmer Lambda 45 UV-Visible spectrophotometer and SPEX Flurolog HORIBA JOBIN VYON fluorescence spectrophotometer with a double-grating 0.22 m SPEX 1680 monochromator and a 450W Xe lamp as the excitation source. The excitation and emission spectra of the complexes were corrected at instrumental function. The photoluminescence lifetime measurements were carried out using a SPEX Flurolog HORIBA JOBIN VYON 1934 D phosphorimeter.

Syntheses

Compound 1: To a stirred solution of TPTA (20mg, 0.058 mmol) in MeOH, $Zn(NO_3)_2{\cdot}6H_2O$ (12.94 mg, 0.044 mmol) in H_2O was added. The resulting solution was left for 2 h stirring and was filtered through celite pad. The filtrate was left for crystallization. The suitable colourless crystals for X-ray analysis were obtained after five days. Yield: 85% (28 mg) based on P. M.P. 216-218 °C. FT-IR data on powder (cm^{-1}): 527, 555, 633, 707, 893, 902, 950, 1035, 1163, 1288, 1316, 1407, 1437, 1588, 1652 and 3461. Anal. Calcd. for $C_{120}H_{196}N_{60}O_{74}P_8S_8Zn_6$: C, 31.61; H, 4.33; N, 18.43; S, 5.62. Found: C, 30.56; H, 4.35; N, 18.67; S, 5.46.

$1_{desolvated}$: This was obtained by heating **1** at 80 °C under high vacuum for 6 h. The formation of desolated phase was confirmed by the TGA and PXRD analysis.

$1_{resolvated}$: This was obtained by the exposure of $\mathbf{1}_{desolvated}$ to the H_2O and MeOH mixture in screw capped vial. This conversion has also been observed by adding one drop of mother liquor to $\mathbf{1}_{desolvated.}$

Compound 2: Compound **2** was prepared by using similar procedure as **1** except $Zn(ClO_4)_2{\cdot}6H_2O$ (22.59 mg, 0.075 mmol) was used instead of the $Zn(NO_3)_2{\cdot}6H_2O$. Yield: 80% (27.94 mg) based on P. M.P. 215-220 °C. FT-IR data on powder (cm^{-1}): 527, 555, 633, 707, 893, 902, 950, 1035, 1163, 1288, 1316, 1407, 1437, 1588, 1652 and 3461. Anal. Calcd. for $C_{120}H_{149}Cl_{12}N_{48}O_{74.50}P_8S_8Zn_6$: C, 30.17; H, 3.14; N, 14.07; S, 5.37. Found: C, 30.25; H, 3.21; N, 14.05; S, 5.35.

Crystallography

Reflections were collected on a Bruker Smart Apex Duo diffractometer at 100 K using MoKα radiation (λ = 0.71073 Å) for all the crystals. Structures were refined by full matrix least-squares against F^2 using all data (SHELX).[2] Crystals of **1** and **2** were diffracted weakly at higher angles and hence a 2θ = 50° cut-off was applied. All the non-hydrogen atoms of metalorganic cages were refined anisotropically and hydrogen atoms were constrained in geometric positions to their parent atoms. Hydrogen atoms of water molecules could not be detected in difference maps and were therefore omitted in the refinement due to the high ambiguity of their positions. The crystals structures of **1** and **2** contain disordered nitrate and perchlorate ions which, in both cases, are disordered across symmetry elements. Ions and water molecules that are not disordered were refined anisotropically, while those that are disordered were treated isotropically and given occupancy factors of 0.5 according to the symmetries of disordered sites. SAME restraints were applied to both disordered nitrate and perchlorates ions, RIGU to the ordered ions and SAME to the disordered ions.

Dielectric and Ferroelectric Measurements

The powder sample of **1** was compacted in the form of discs (of approximately 10 mm diameter and 1 mm thickness) to measure dielectric properties. The compacted discs were subsequently electrode using aluminium adhesive foils for both measurements. The dielectric characteristics for **1** were measured using the Novocontrol, Dielectric Spectrometer.

The ferroelectric hysteresis loops in **1** were measured on single crystal of thickness 0.5 mm and area of 2.5 mm^2 (2.5 mm X 1mm) by using Sawyer-Tower circuit. The measurements

pertaining to the polarization and fatigue cycles were recorded using hysteresis loop analyser (TF Analyser 2000E, aixACCT Germany). Leakage current was measured dynamically for various voltage steps during the hysteresis loop measurements.

Second Harmonic Generation

The measurement of the powder second harmonic generation was carried out by using the method of Kurtz and Perry.[3] The fundamental wavelength is 1064 nm generated by a Q-switched Nd:YAG laser with a frequency doubling at 532 nm. The samples were filled into a capillary tube and a powdered urea sample was used as the reference.

Calculation of Dipole Moment

To calculate the polarization of the system we have done the theoretical optimization by using the Gaussian 09 program.[4] The cationic cage segment was considered as low layer and twenty six molecules of H_2O and twelve nitrate anions were selected as high layer to perform ONIOM calculation. The calculation for high layer was done by DFT methods and semi-empirical method (PM6) was used for the lower layer.

Characterization and Crystal Structure for TPTA, 1 and 2

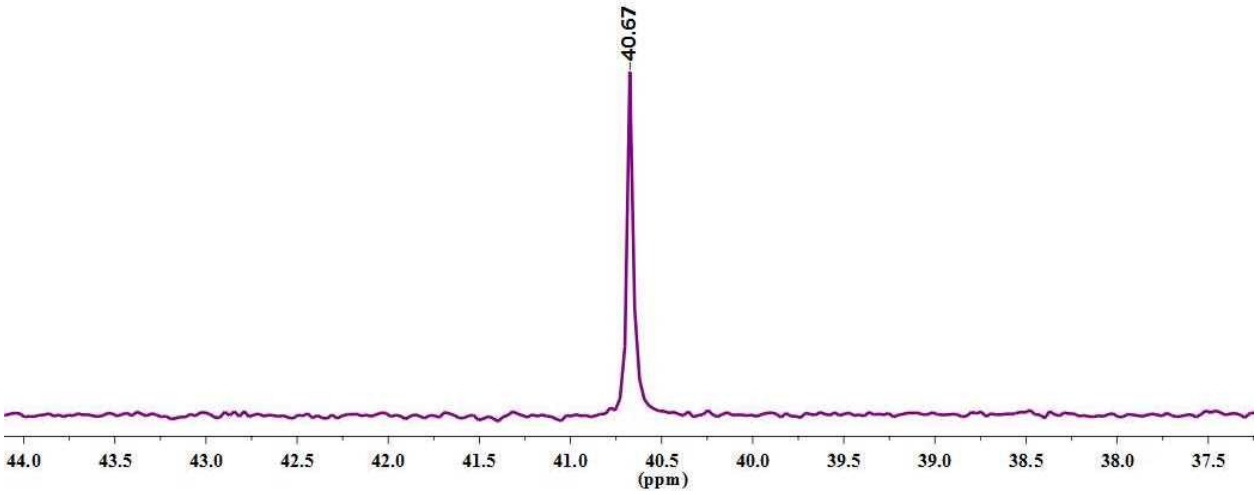

Figure S1: ^{31}P NMR spectrum of ligand TPTA.

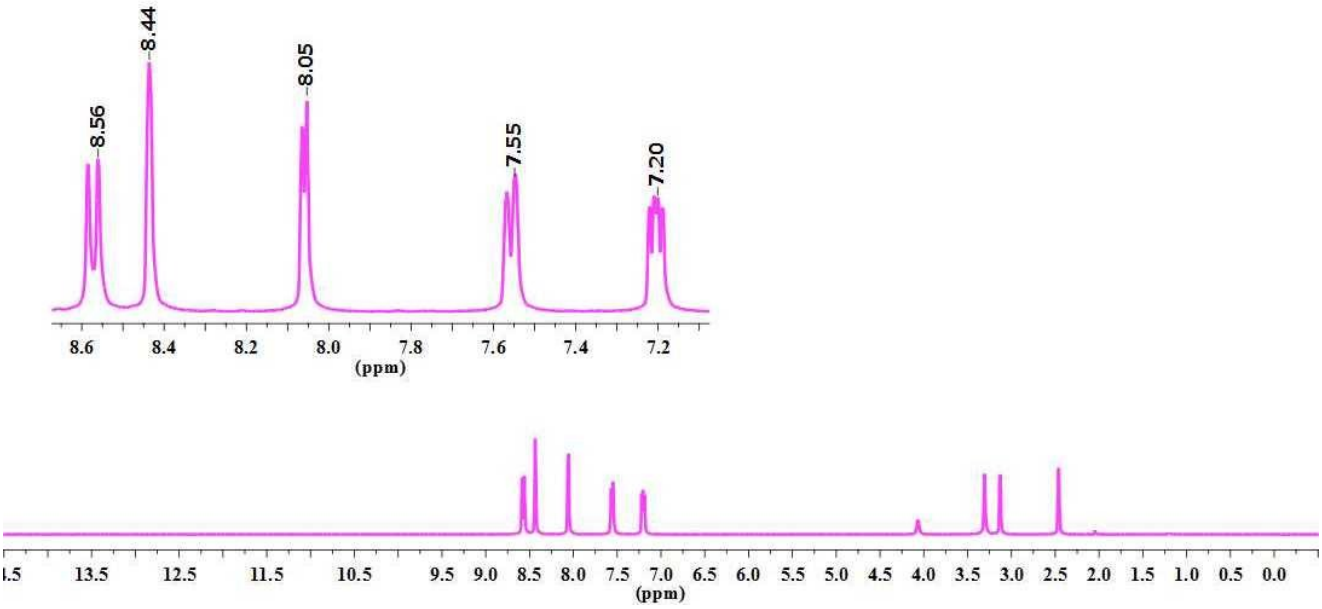

Figure S2: ^{1}H NMR spectrum of the ligand TPTA.

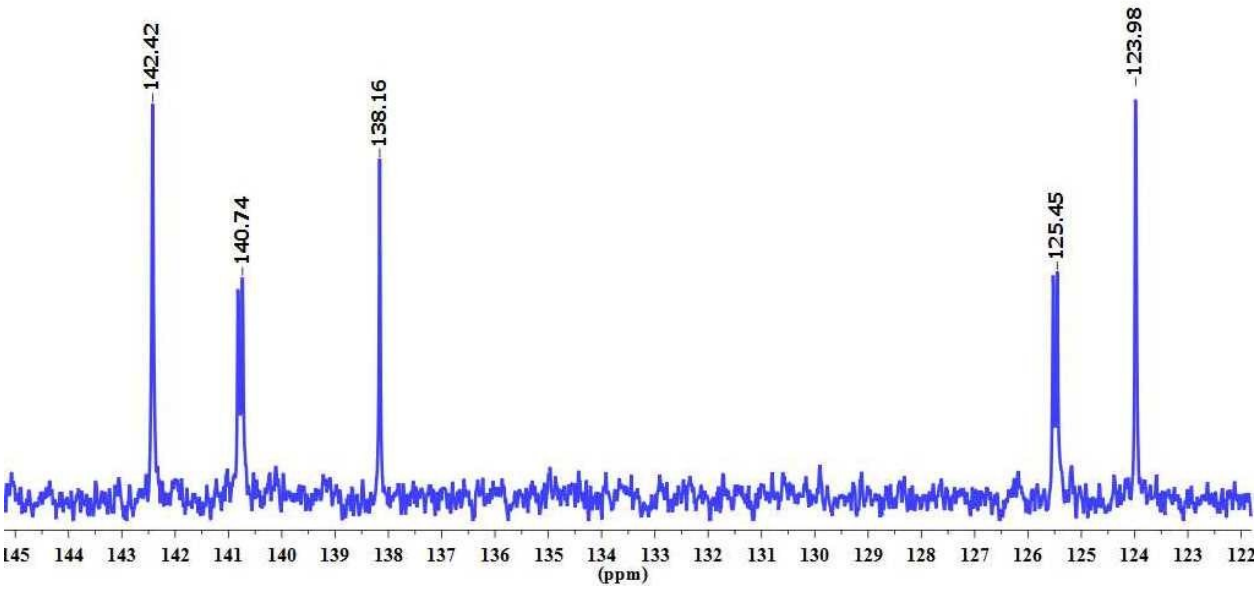

Figure S3: ^{13}C NMR spectrum of ligand TPTA.

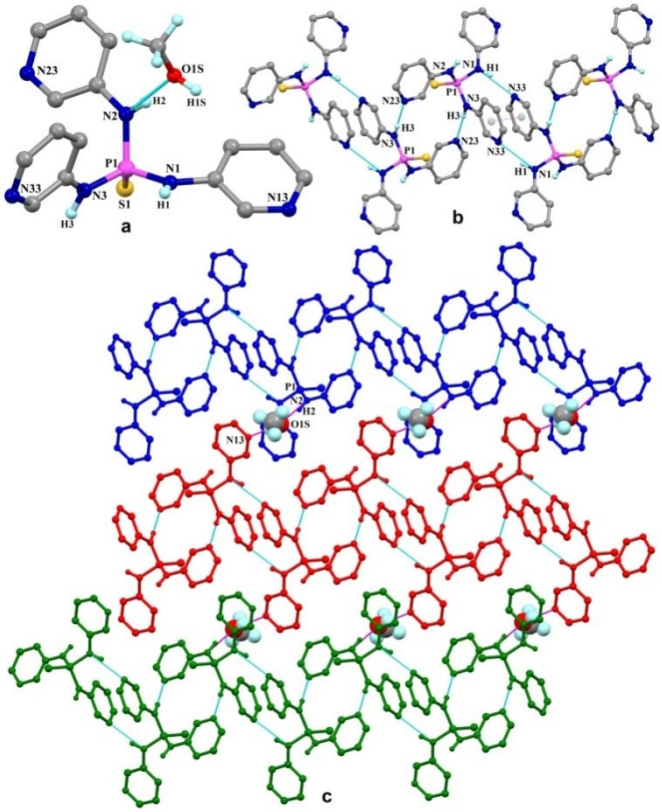

Figure S4: Crystal structure of ligand TPTA: (a) single molecule, (b) showing hydrogen bonding thorough NH proton and $N_{pyridyl,}$ (c) two dimensional network formed by the hydrogen bonding.

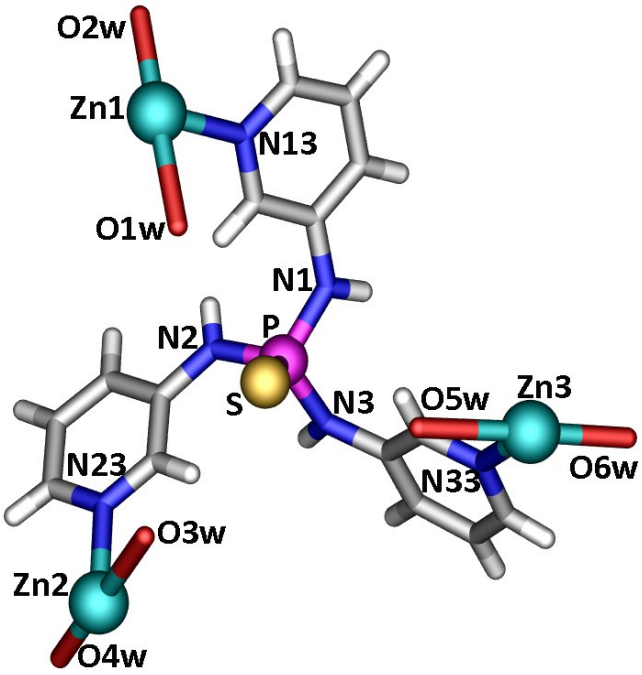

Figure S5: Diagram showing the connection of TPTA ligand with zinc centre in **1** and **2**.

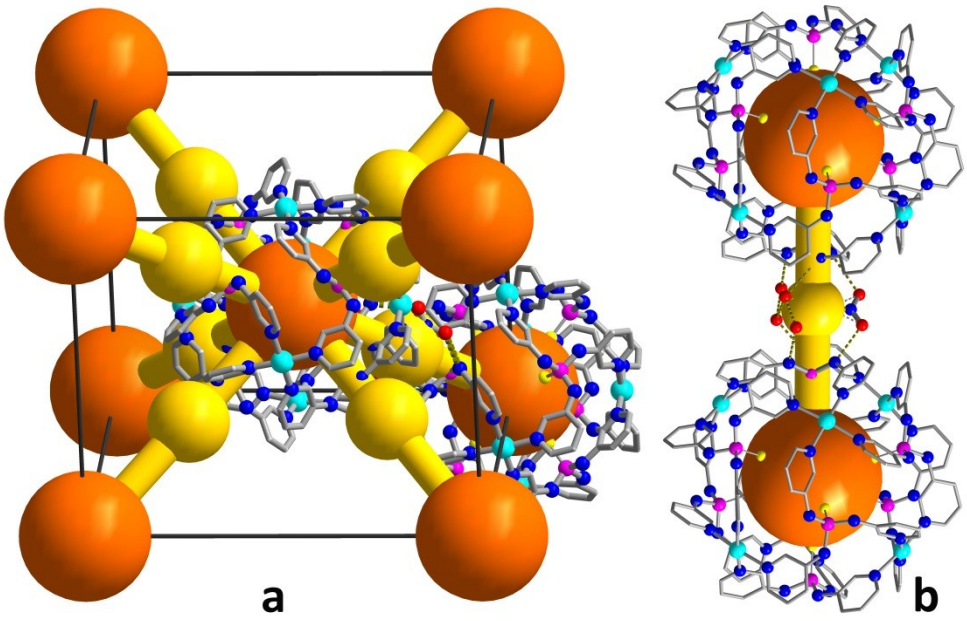

Figure S6: Formation of an interesting H-bonded network in **1** involving the $P(NH)_3$ units and ordered molecules of solvated water and nitrate ions. These interactions were found at all the eight $P(NH)_3$ units of the cage.

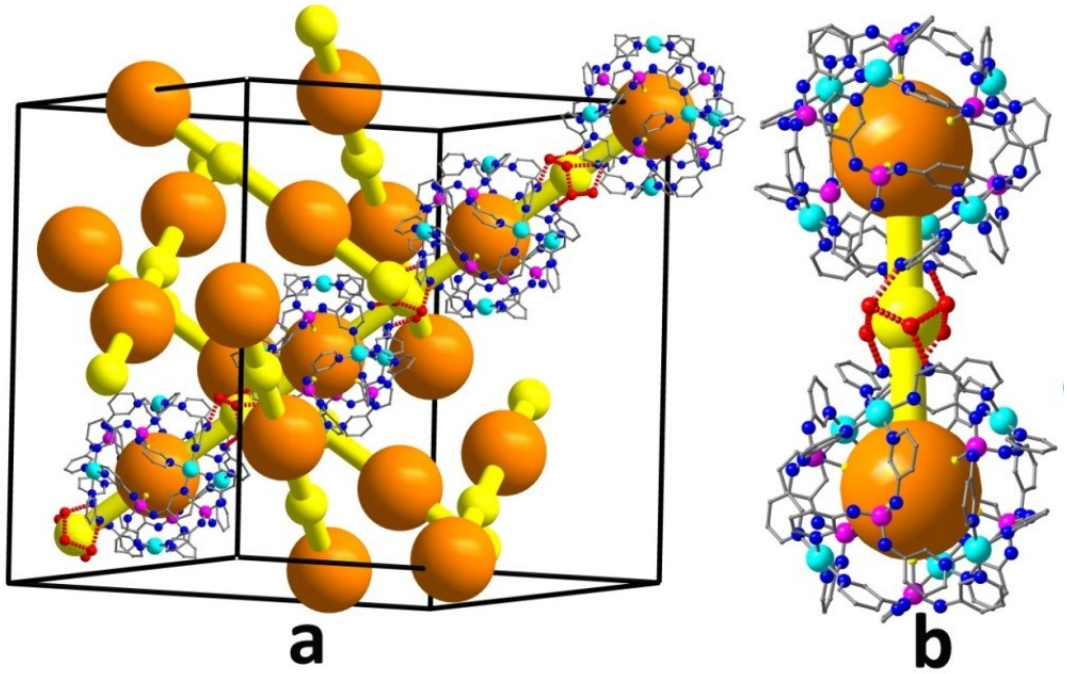

Figure S7: Formation of an interesting water hexamer in **2** that links two cages via $P(NH)_3$ units, forming linear chains of connected cages throughout the crystal. The other $P(NH)_3$ groups are linked by disordered perchlorates (Figure S21).

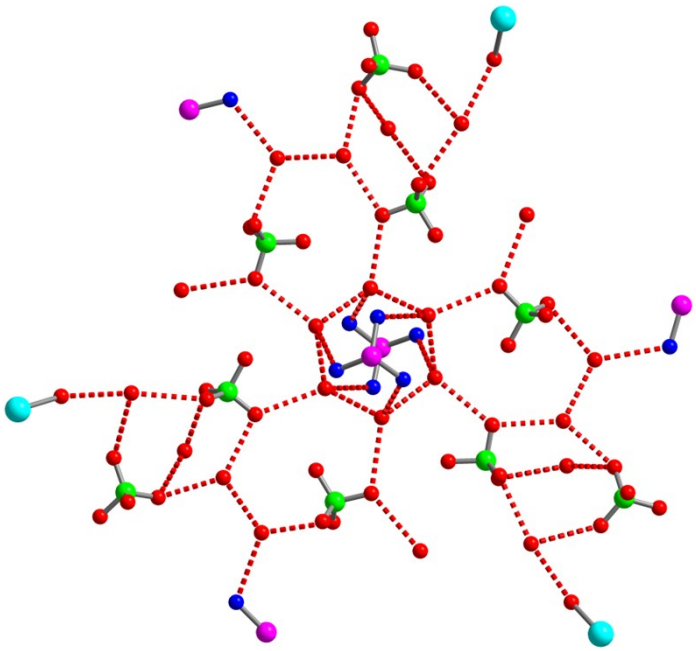

Figure S8: Close view of the H-bonding of the water hexamer in **2** with the two adjacent $P(NH)_3$ units and ordered part of the perchlorate anions.

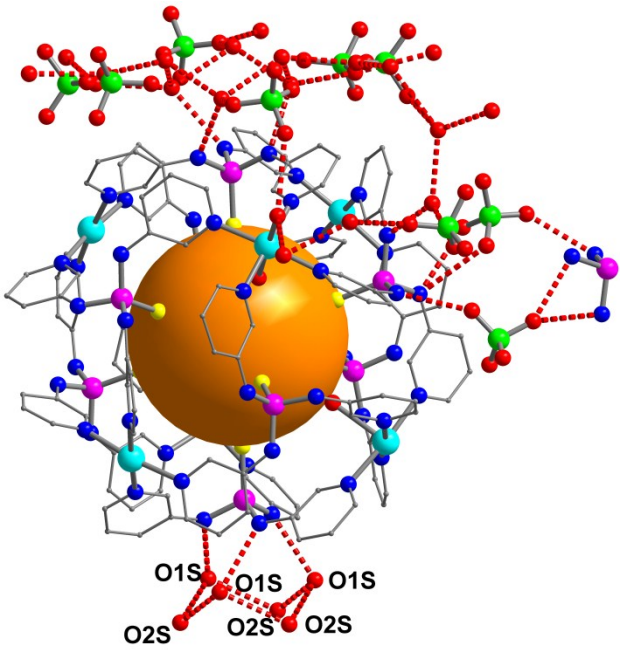

Figure S9: Arrangement of ordered and disordered perchlorate anions around a single cage core in **2** that are H-bonded with six $P(NH)_3$ units and solvate molecules**.**

Table S1: Crystallographic Data.

Compound	**TPTA**.MeOH	**1**	**2**
Chemical formula	$C_{16}H_{19}N_6OPS$	$C_{120}H_{196}N_{60}O_{74}P_8S_8Zn_6$	$C_{480}H_{726}Cl_{48}N_{192}O_{315}P_{32}S_{32}Zn_{24}$
Formula weight	374.40	4559.82	19513.92
Temperature	100(2) K	100(2) K	100(2) K
Crystal system	Triclinic	Tetragonal	Cubic
Space group	P-1	I4	I-43d
a (Å); α (°)	8.937(14); 85.10(3)°	21.096(9); 90	44.497(4); 90
b (Å); β(°)	9.663(15); 84.91(3)°	21.096(9); 90	44.497(4); 90
c (Å); γ (°)	11.854(18); 63.27(3)°	24.031(13); 90	44.497(4); 90
V (Å^3); Z	909.4(2) ; 2	10694.7(11); 2	88103(24); 4
ρ (calc.) mg m^{-3}	1.367	1.416	1.471
μ(Mo K_α) mm^{-1}	0.283	0.894	1.014
$2\theta_{max}$ (°)	56	50	50
R(int)	0.0289	0.0648	0.1268
Completeness to θ	99.7 %	99.8 %	99.4 %
Data / param.	4512 / 228	8788 / 621	12925/849
GOF	1.036	1.051	1.011
R1 [F>4σ(F)]	0.0310	0.0773	0.0887
wR2 (all data)	0.0832	0.2369	0.2870
max.peak/hole (e.Å^{-3})	0.562/-0.537	1.608 /-0.498	1.229/-1.198

Table S2: Hydrogen bond table for TPTA, **1** and **2**

Compound	D-H...A	d(H...A)Å	d(D...A)Å	<(DHA) °
TPTA	N(1)-H(1)...N(33)#1	2.23	2.9926(16)	144.6
	N(2)-H(2)...O(1S)	1.91	2.7703(15)	164.6
	N(3)-H(3)...N(23)#2	2.09	2.9675(16)	173.4
	O(1S)-H(1S)...N(13)#3	1.92	2.7577(16)	172.4
	#1 -x+2,-y+1,-z+1 #2 -x+1,-y+2,-z+1 #3 -x+2,-y+1,-z+2			
1	N(2)-H(2)...O(103)#1	2.10	2.942(14)	165.5
	N(3)-H(3)...O(11)	2.06	2.885(15)	161.7
	N(4)-H(4)...O(13)#2	2.03	2.890(13)	173.4
	N(5)-H(5)...O(101)#3	2.09	2.925(10)	164.9
	N(6)-H(6)...O(104)#4	2.06	2.909(13)	167.3
	#1 -y+3/2,x+1/2,z+1/2 #2 -x+1/2,-y+3/2,z-1/2			
	#3 y-1/2,-x+3/2,z-1/2 #4 y+1/2,-x+3/2,z-1/2			
2	N(1)-H(1)...O(2S)#1	2.05	2.910(12)	163.7
	N(2)-H(2)...O(5S)	2.08	2.938(11)	165.4
	N(3)-H(3)...O(6S)	2.15	2.966(18)	153.9
	N(4)-H(4)...O(9A)#2	2.17	3.045(18)	173.4
	N(4)-H(4)...O(10A)#2	2.54	3.14(3)	126.6
	N(4)-H(4)...O(10B)#2	2.03	2.85(3)	154.1
	N(5)-H(5)...O(13A)#3	2.02	2.88(3)	163.4
	N(5)-H(5)...O(13B)#3	2.06	2.914(18)	164.2
	N(7)-H(7)...O(14A)#4	1.92	2.79(2)	169.6
	N(7)-H(7)...O(14B)#4	2.26	3.12(3)	166.0
	N(7)-H(7)...O(15B)#4	2.54	3.24(4)	137.5
	C(56)-H(56)...O(13A)#5	2.56	3.29(3)	133.3
	N(6)-H(6)...O(11A)	2.01	2.886(17)	171.2
	N(6)-H(6)...O(9B)	2.37	3.19(3)	154.4
	N(8)-H(8)...O(8S)#6	2.01	2.87(3)	166.0
	#1 -x+1,y+1/2,-z+3/2 #2 z-3/4,-y+7/4,-x+5/4			
	#3 -x+1/4,z+1/4,-y+7/4 #4 y-1/2,-z+3/2,-x+1			
	#5 z-1/4,y-1/4,x+3/4 #6 -z+5/4,-y+7/4,x+3/4			

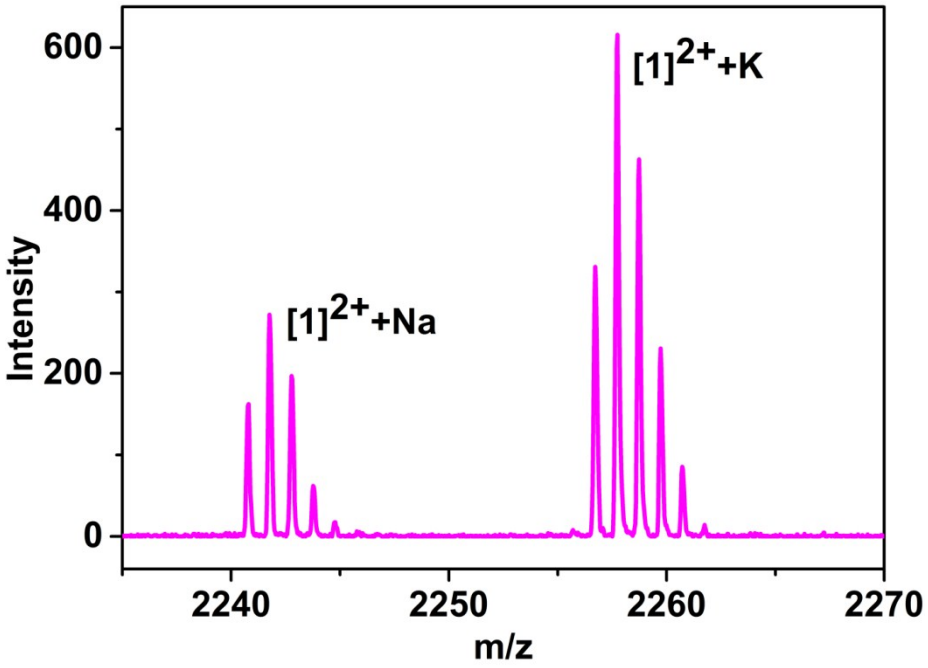

Figure S10: MALDI-TOF mass spectrum of **1**.

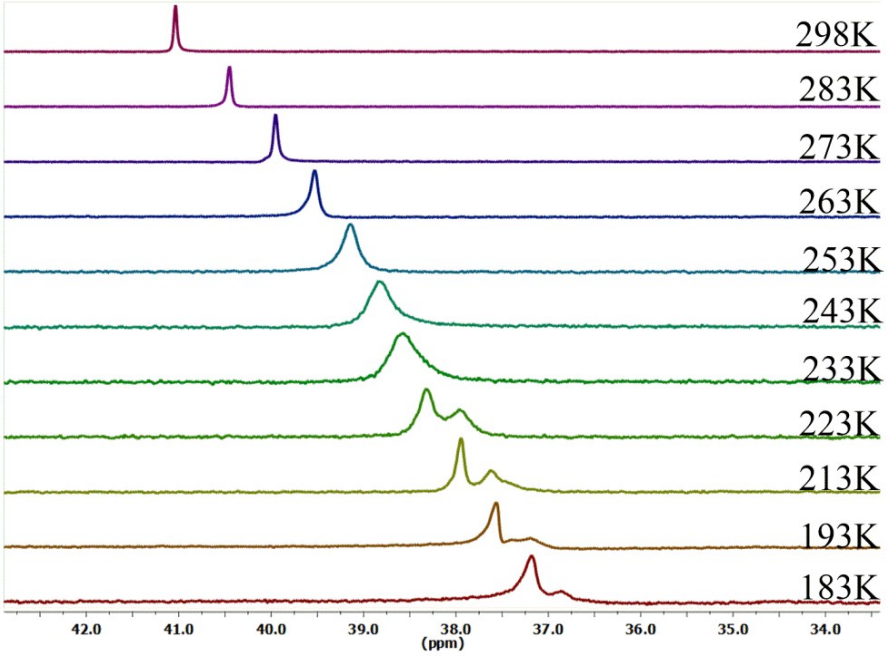

Figure S11: Variable temperature ^{31}P NMR spectrum of **1** suggesting the presence of two enantiomers in the solution.

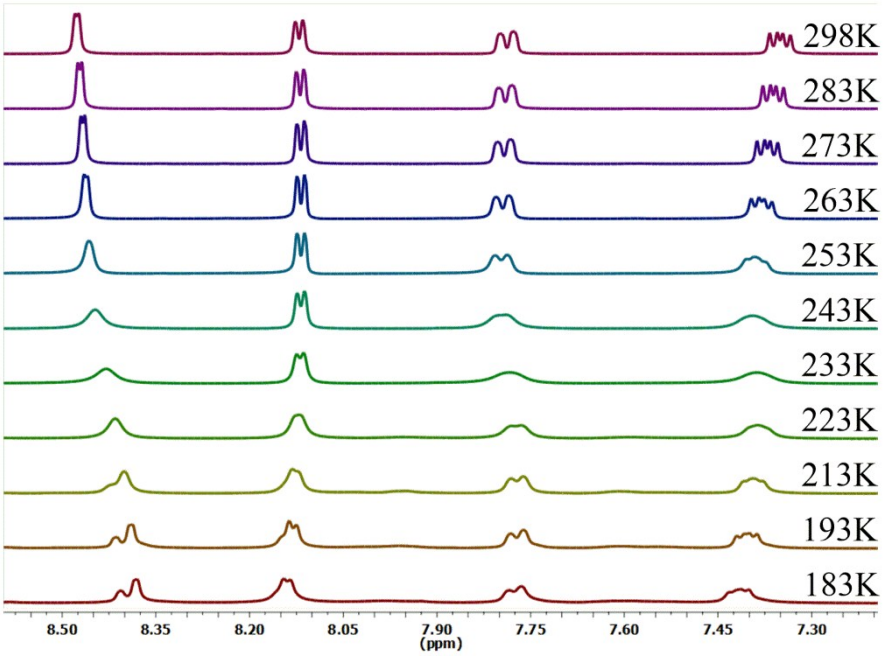

Figure S12: Variable temperature ^{1}H NMR spectrum of **1**: Broadening in the signals suggesting the presence of two enantiomers in the solution

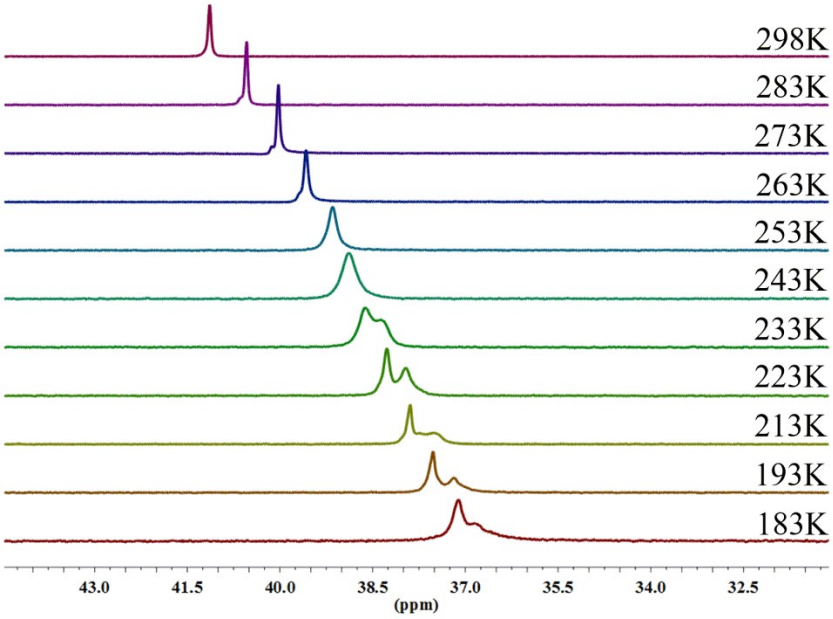

Figure S13: Variable temperature ^{31}P NMR spectrum of **2** suggesting the presence of two enantiomers in the solution.

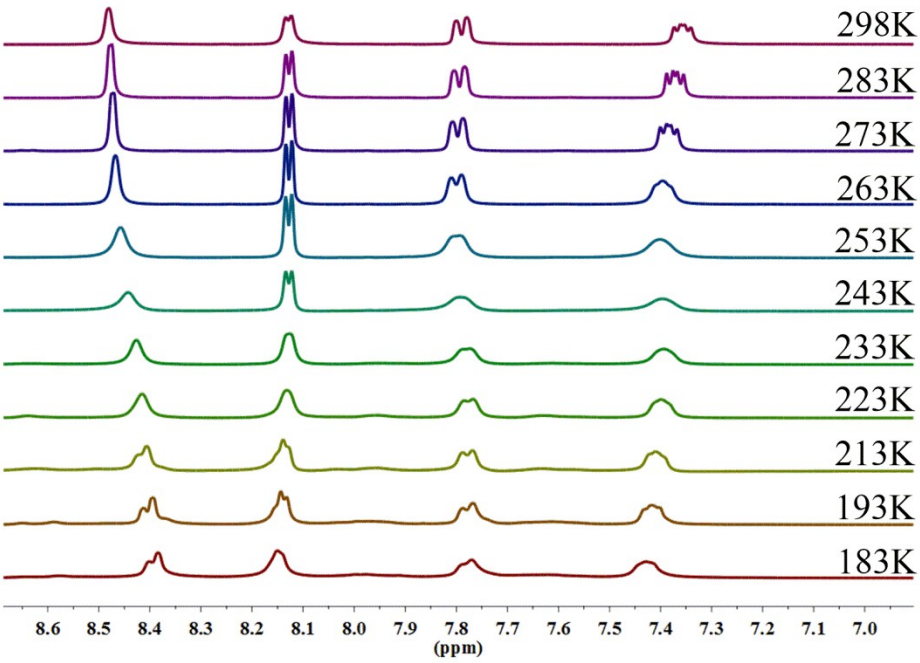

Figure S14: Variable temperature ^{1}H NMR spectrum of **2**: Broadening in the signals suggesting the presence of two enantiomers in the solution

Ferroelectric and Dielectric measurements

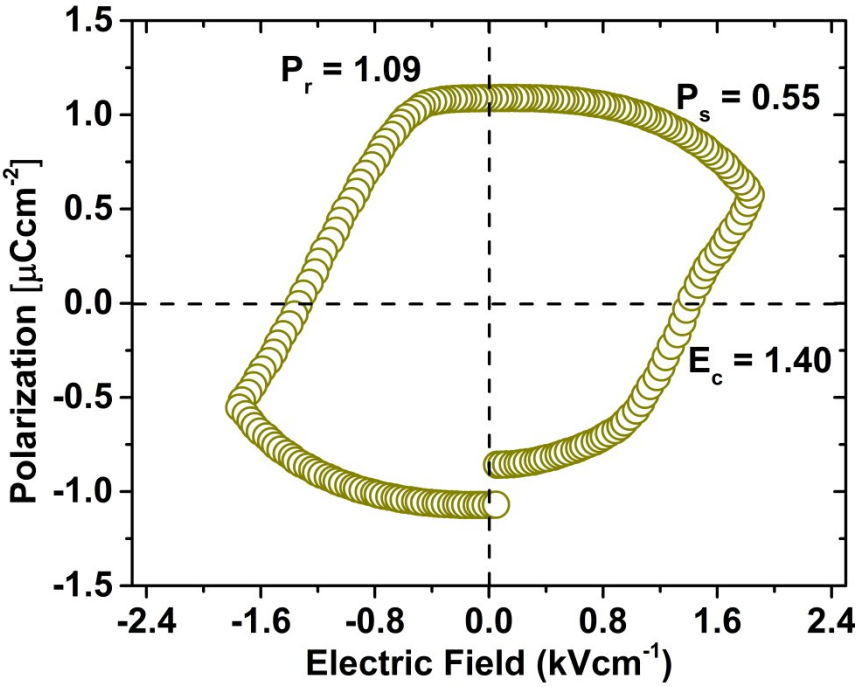

Figure S15: Ferroelectric loop measurements on **1** at 1Hz.

Table S3: Current data obtained after subjecting the single crystal of **1** to an increasing dc field.

Applied Voltage	Current (μA)
1.5 V	45.69
5 V	46.11
9 V	46.18
15 V	46.27
21 V	46.29
30 V	46.51
45 V	46.64
55 V	46.65
75 V	46.70
85 V	46.75
95 V	46.78
125 V	46.40
225 V	46.56
325 V	46.70
425 V	46.86
525 V	46.90
825 V	47.01
925 V	47.11
1k V	47.16

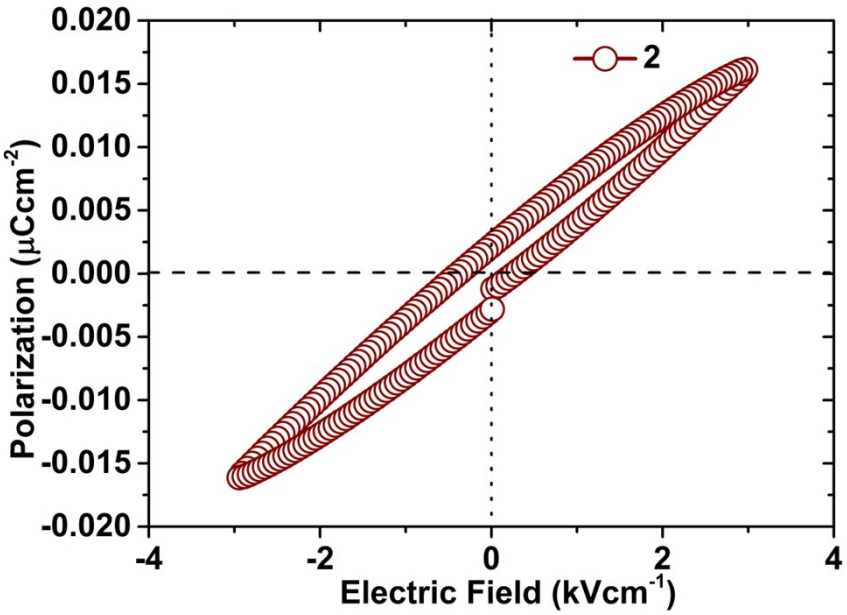

Figure S16: Ferroelectric loop measurements on **2** at 1Hz.

Table S4: Remnant polarization and the coercive field of some recent reported metal-organic assemblies.*

S.N.	Material	P_r(μCcm^2; T (K)	E_c (kVcm^{-1})	Measurement Sample	Emission	Reference
1	$[(CH_3)_3NOH]_2[KFe(CN)_6]$	0.58; RT	5.7	Crystal	Non emissive	7
2	$[(CH_3)_3NOH]_2[KFe(CN)_6]$	1.25; RT	233	Thin film	Non emissive	7
3	$Ca_6^{II}\{Cu^{II}_{24}[(S,S)hismox]_{12}(OH_2)_3\}\cdot 212H_2O$	1.06; 103	-	Crystal	Non emissive	8
4	$(CH_3NH_3)_12\{Cu^{II}_{24}[(S,S)hismox]_{12}(OH_2)_3\}\cdot 178H_2O$	1.06; 103	-	Crystal	Non emissive	8
5	$[NH_4][Zn(HCOO)_3]$	0.5; 163	-	Pellet	Non emissive	9
6	$\{[Cu_2L_4(H_2O)_2]\cdot(ClO_4)_4\cdot(H_2O)_5\cdot(CH_3OH)\}_\infty$	1.8; RT	16	Pellet	Non emissive	10
7	$(\{[CuL^1_2(H_2O)_2]\cdot(NO_3)_2\cdot(H_2O)_{1.5}\cdot(CH_3OH)\}_\infty)$	27.96; RT	5.9	Pellet	Non emissive	11
8	$[\{Ni_4L_8(H_2O)_8\}\supset 9(H_2O)]\cdot(NO_3)_8\cdot 25(H_2O)$	29.50; RT	8.60	Pellet	Non emissive	12
9	$[\{Co_4L_8(H_2O)_8\}\supset 9(H_2O)]\cdot(NO_3)_8\cdot 27(H_2O)$	29.50; RT	8.60	Pellet	Non emissive	12
10	$\{[Zn_6(H_2O)_{12}][TPTA]_8\}(NO_3)_{12}\cdot 26H_2O$	1.20; RT	0.86	Crystal	Blue emissive	Present Report

*A similar comparison of the ferroelectric properties of several small molecules, polymeric and metal-organic materials have been given in the reference 11.

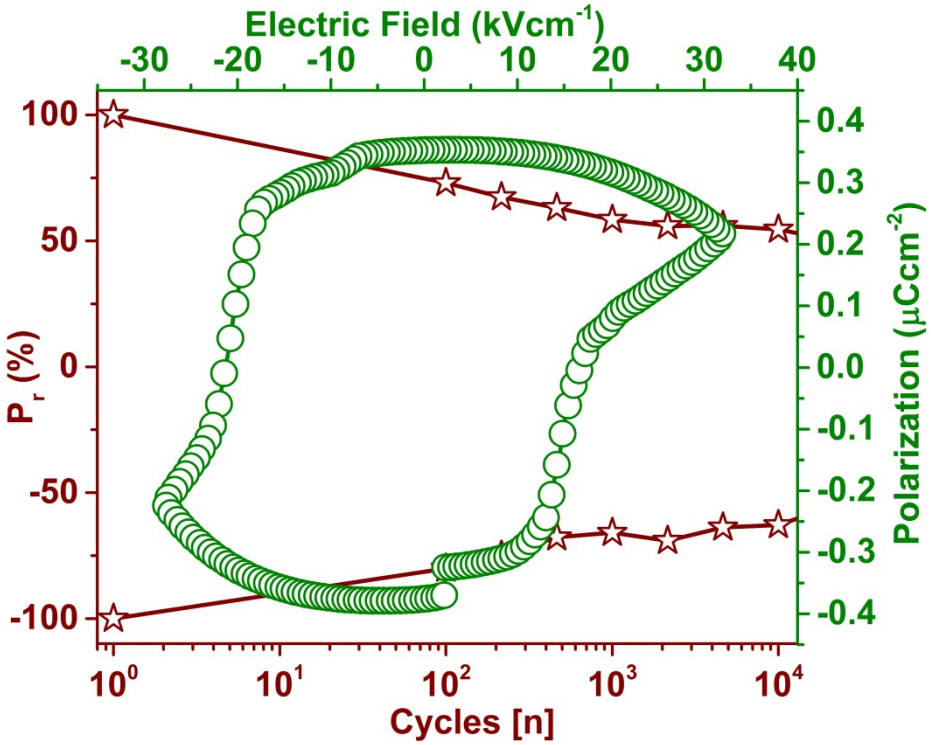

Figure S17: Ferroelectric fatigue measurements on **1** and the corresponding P-E loop at 0.1Hz after 10^5 cycles.

Structural analysis and possible origin of polarization of 1:

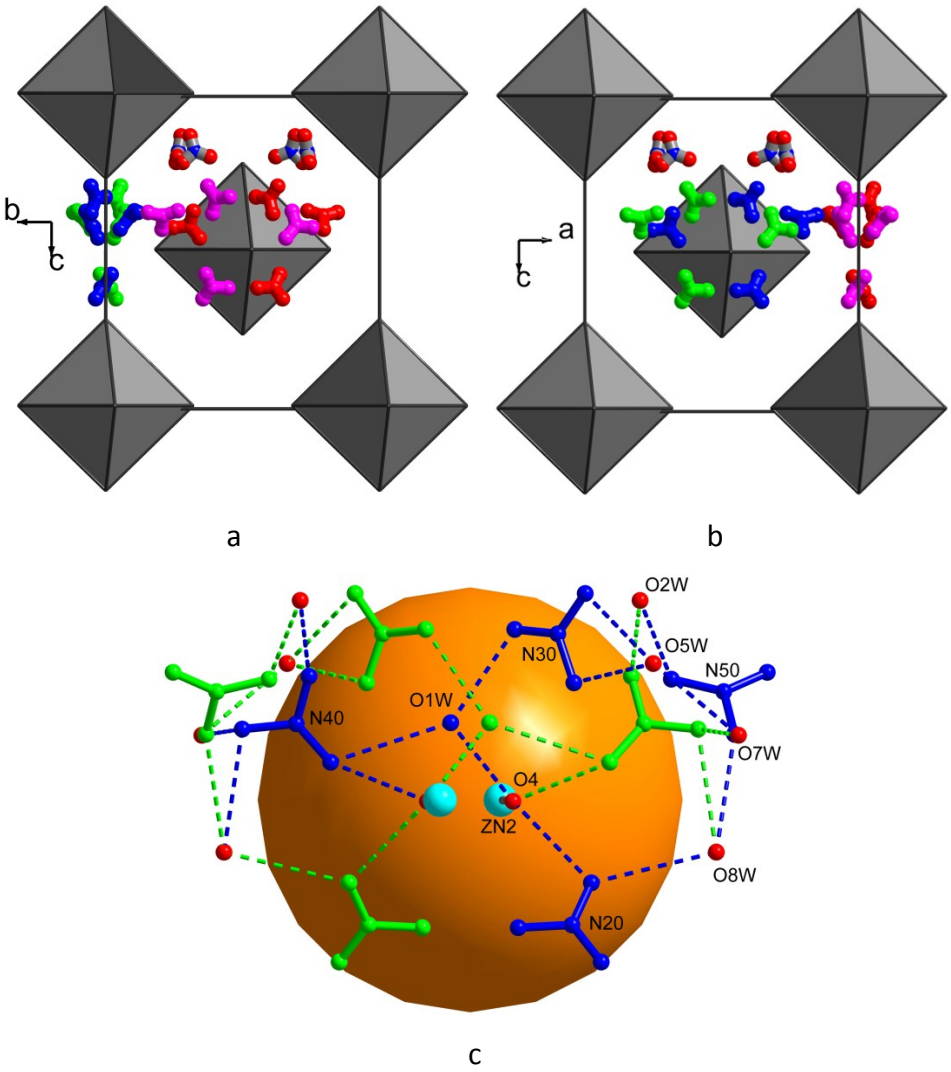

Figure S18: Distribution of nitrate anions in **1** viewed along *a* (figure a) and *b* (figure b) axes within the framework of coordination polyhedra (depicted as grey octahedra, Zn ions mark the corners). The ordered nitrate ions have been shown in regular colours; N: Blue, O: Red, bonds: Grey (along *c* axis), disordrered nitrates has been shown in different colours pink and red spheres (along *a*-axis) and blue and green spheres (along *b*-axis). (c) Closer view of the interaction of disordered nitrate ions with solvate water molecules in **1**. The orange sphere depicts the metal-organic cage.

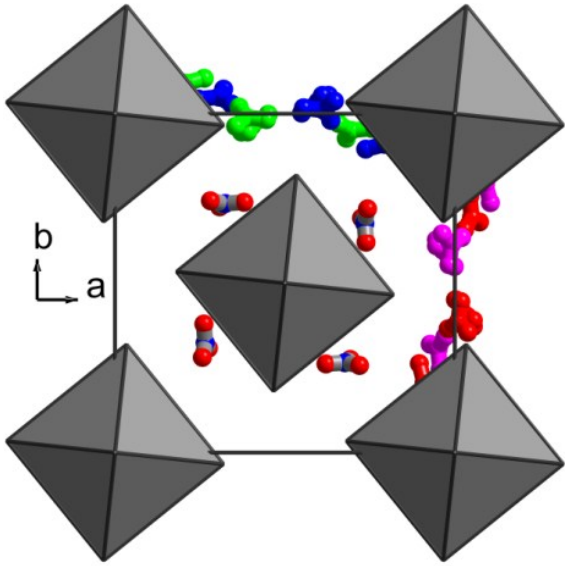

Figure S19: Distribution of nitrate anions in **1** viewed along *c* axis (left) within the framework of coordination polyhedra (depicted as grey octahedra, Zn ions mark the corners). Disordered sets of nitrate ions are depicted in purple/red and blue/green, respectively

Dielectric Measurements on the crystals of 1*

*The variable (biased) nature of electric dipoles along the different axes of a crystal can be derived from obtaining the information on the dielectric constants at a given direction. A single crystal of **1** electroded with Ag-paint was subjected to capacitance measurements in an LCR meter and the obtained values are given in the table S3. We did not attempt to convert these capacitance values to dielectric constants as crystals were irregular in shape and their dimensions were varying at different ends. Since the value of capacitance is directly proportional to the dielectric constant, the observed capacitance values are the measure of the dipole moments at different directions of the crystals. Notably the values of capacitance, at any given frequency, is very low along the c-axis and are comparably much higher along a- and b-axes confirming the polarization in **1** is operating parallel to the principal axis.

Table S5: Measurement of capacitance values on the single crystals of **1** along different axes at room temperature.

Crystal Dimensions (mm)		Frequency (Hz)	Capacitance (pF)		
			a-axis	b-axis	c-axis
Crystal I	1.54 × 1.88 × 1.48	100	183	269	20
		1000	90	120	11.7
		10000	43	42	8
		100000	15	14	5
		1000000	6	5	4
Crystal II	1.98 × 1.46 × 2.10	100	228	216	33
		1000	145	129	15
		10000	73	69	9
		100000	23	25	5
		1000000	5	5	4
Crystal III	1.26 × 1.03 × 2.62	100	123	104	51
		1000	60	59	25
		10000	28	27	12
		100000	10	10	6
		1000000	5	5	3
Crystal IV	1.56 × 1.00 × 2.10	100	152	104	21
		1000	86	75	9
		10000	58	25	5
		100000	25	17	4
		1000000	7	5	3

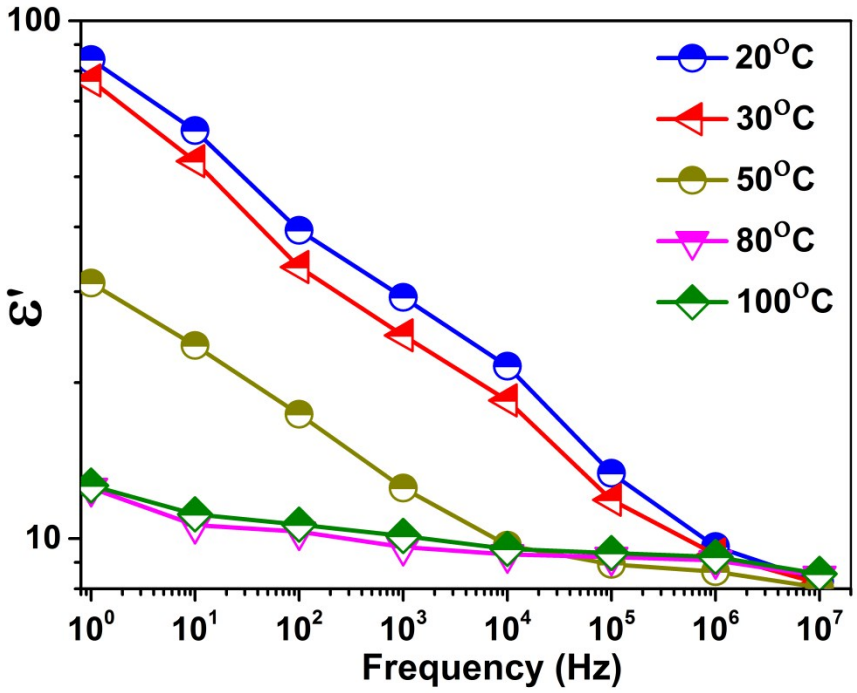

Figure S20: Frequency dependent dielectric constant of **1** at various temperatures.

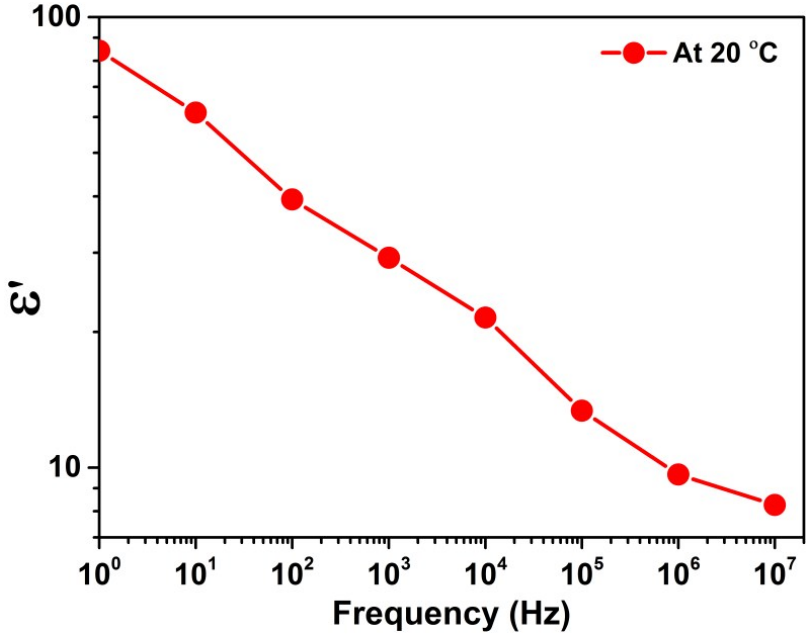

Figure S21: Frequency dependent dielectric constant of **1** at 20 °C.

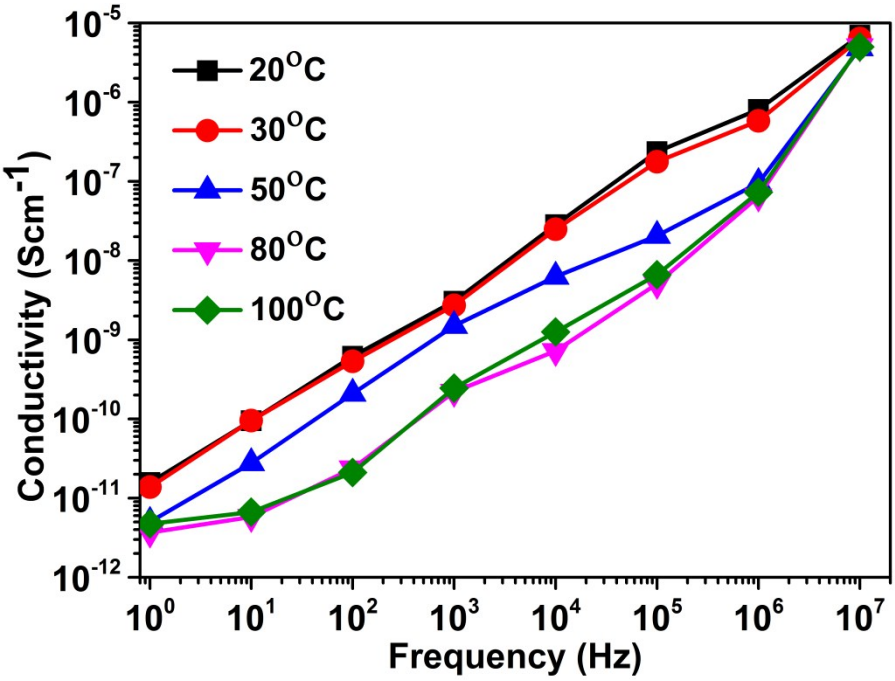

Figure S22: Conductivity vs frequency plot for **1**.

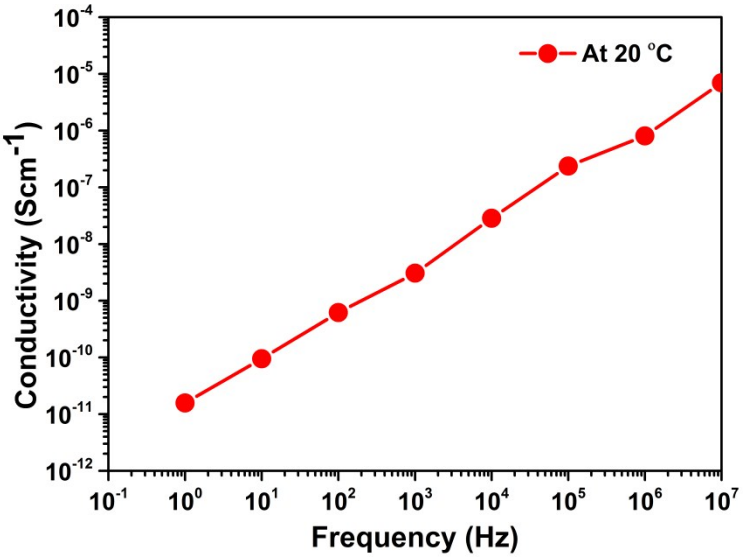

Figure S23: Conductivity vs frequency plot for **1** at 20 °C

Solvent dependent studies: Ferroelectric, TGA, IR, XRD and NMR data

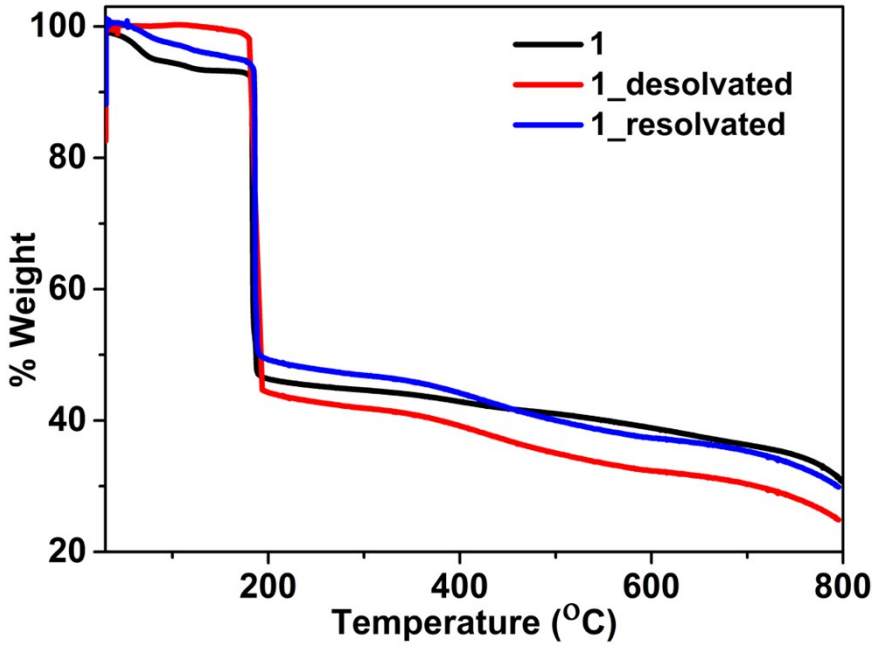

Figure S24: Thermogravimetric analysis (TGA) plot for **1**, $\mathbf{1}_{desolvated}$ and $\mathbf{1}_{resolvated}$.

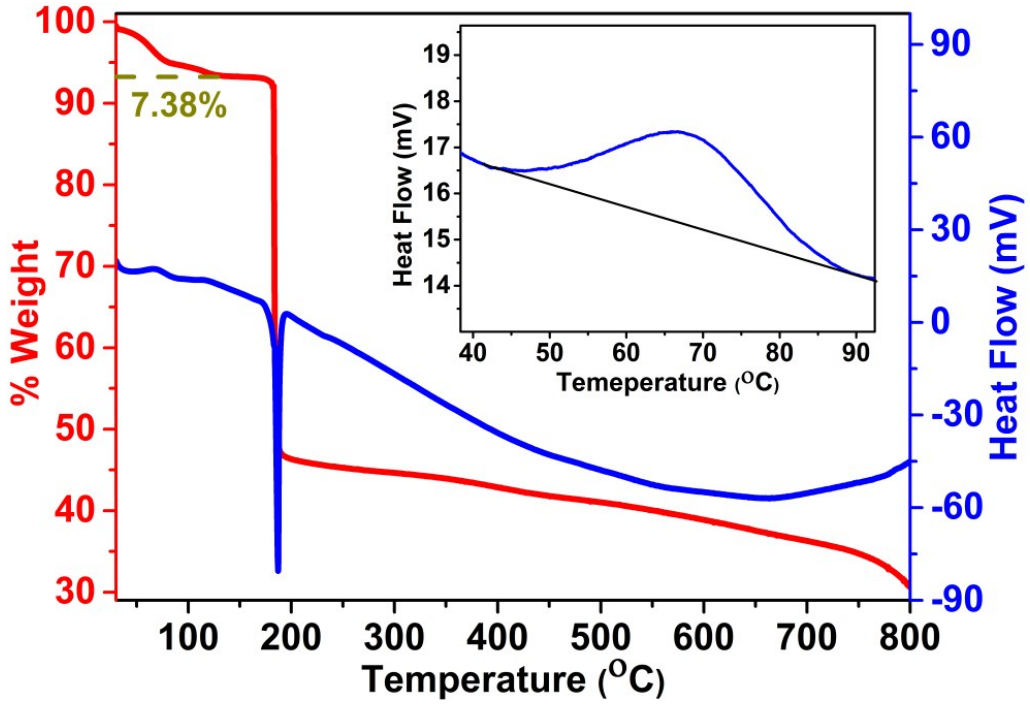

Figure S25: TGA-DTA plot for **1**.

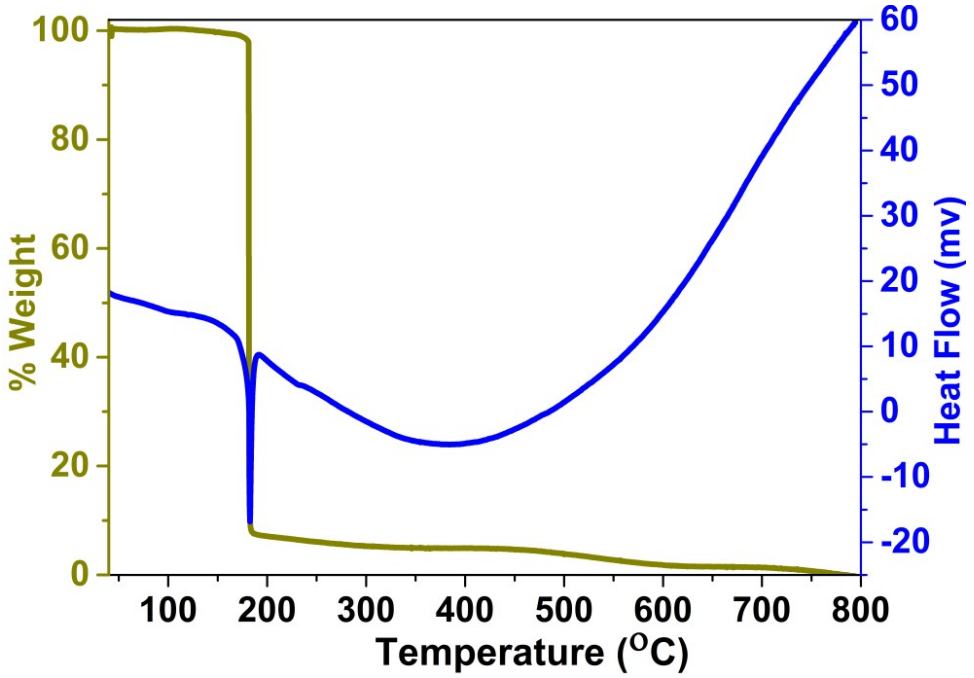

Figure S26: TGA-DTA plot for $\mathbf{1}_{desolvated}$.

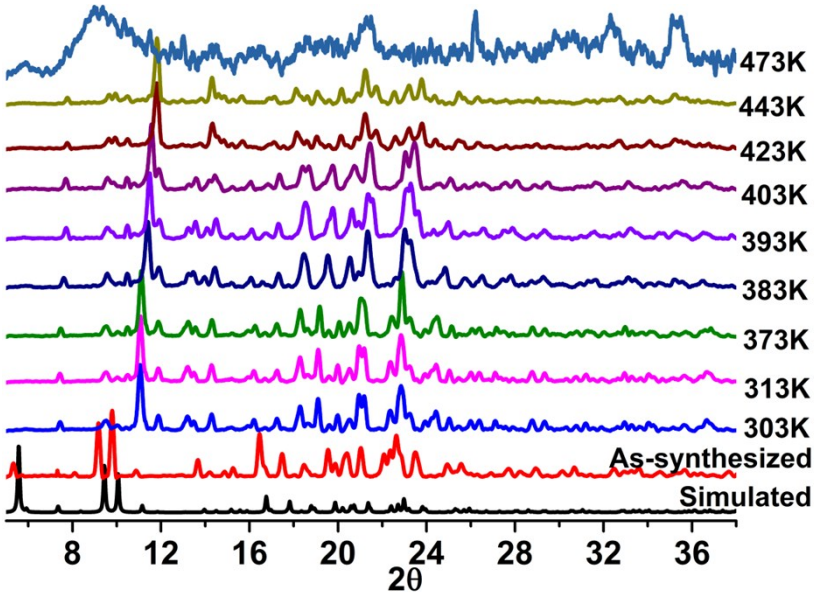

Figure S27: Variable Temperature PXRD pattern of **1**. The crystallinity of the sample was retained up to 120 °C.

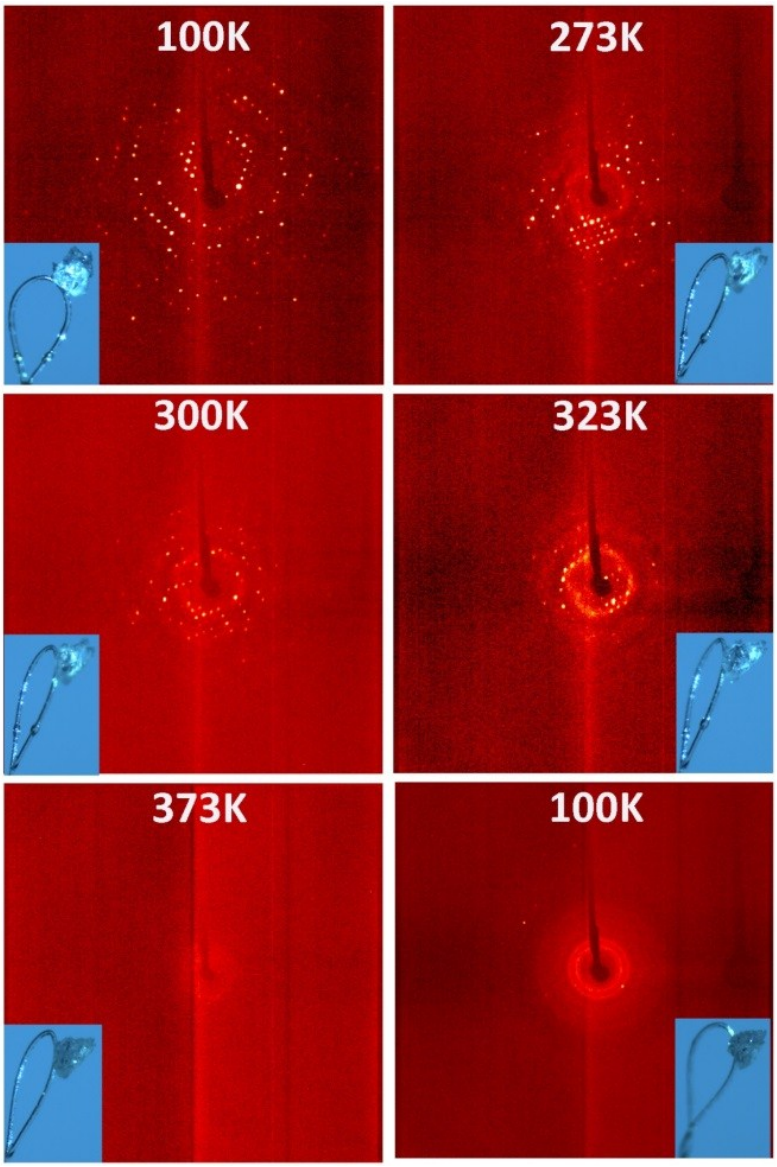

Figure S28: Diffraction spots of the single crystal of **1** during the desolvation and resolvation (the frame at the bottom right corner).

Table S6: Unit cell parameter data for **1** at various temperatures

Compound	*T* (K)	a (Å)	c (Å)	V (Å^3)
1	100	21.12(9)	24.04(13)	11285
	273	21.47(10)	23.74(13)	10946
	298	21.35(7)	23.96(9)	10919
	323	21.37(7)	23.87(8)	10909

Solid State NMR Spectra

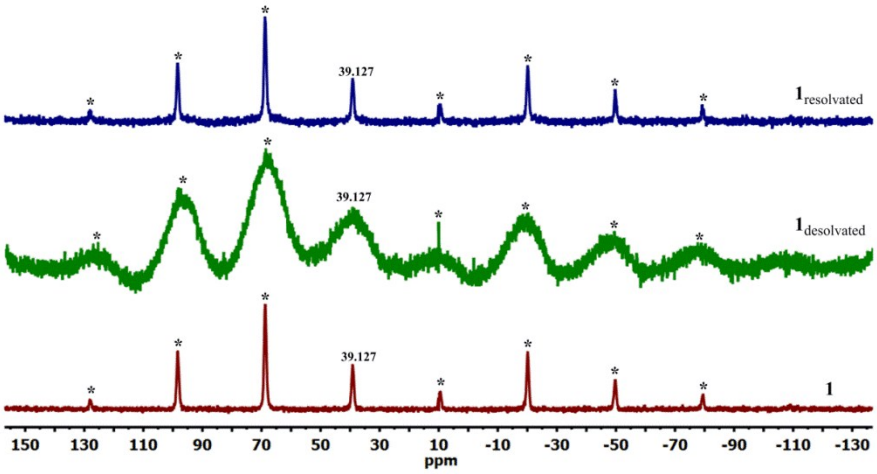

Figure S29: ^{31}P-NMR of **1** (brown), $\mathbf{1}_{desolvated}$ (green), and $\mathbf{1}_{resolvated}$ (blue). Peaks denoted with asterisks are spinning side bands.

The solid-state NMR spectra were measured on a Bruker Advance DSX 500 spectrometer operating at 202.40 MHz for ^{31}P. All spectra were collected using a 4 mm triple resonance probe and zirconia rotors. The ^{31}P{^{1}H} MAS NMR spectra were measured at a MAS rate of 10 kHz with ^{1}H TPPM decoupling during acquisition at an *rf* field of *ca.* 83 kHz. A ^{31}P π/3 pulse length of 2.1 μs with a recycle delay of 120.0 s was used.[5] The solid state CP-MAS ^{31}P-NMR spectra of the bulk samples of **1**, $\mathbf{1}_{desolvated}$ and $\mathbf{1}_{resolvated}$ gave almost identical peak patterns consisting of a sole signal due to ligand phosphorus atom at 39.13 ppm (Figure S28).

Photophysical Studies

Table S7: Quadratic non-linear optical data.[6]

Compound	SHG Intensity
1	30 mV
$\mathbf{1}_{desolvated}$	15 mV
$\mathbf{1}_{resolvated}$	35 mV
Urea	135mV

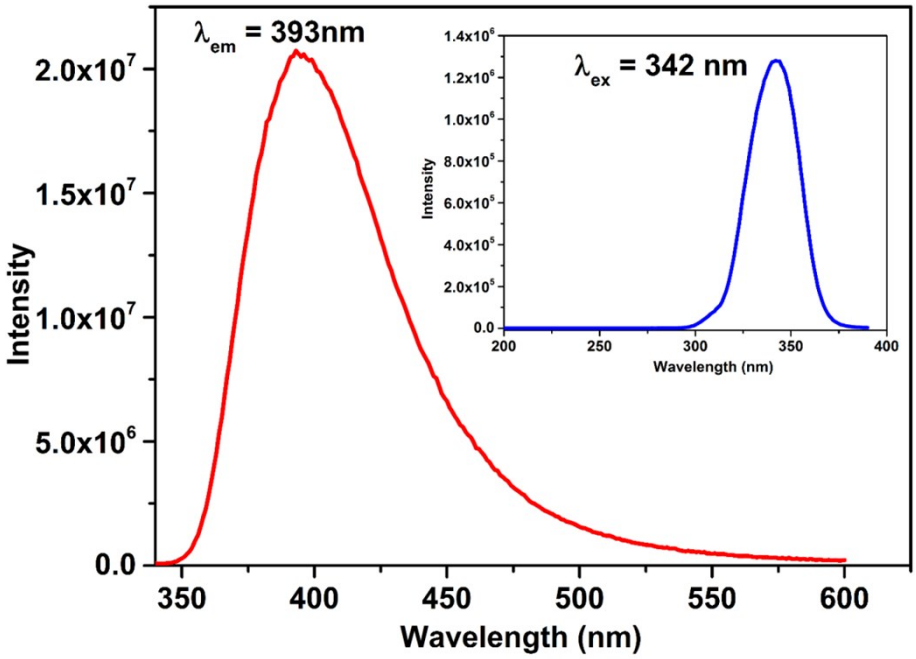

Figure S30: Fluorescence peak profile of **2** in the solid state; the inset shows the excitation spectrum of **2** at 342 nm.

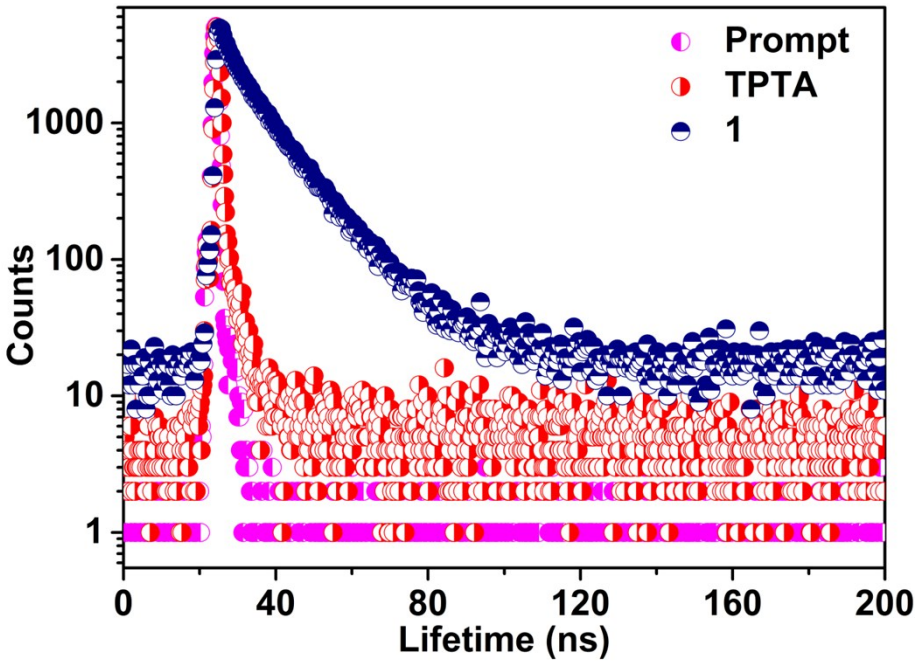

Figure S31: Luminescence decay profile for **1** (navy blue), TPTA (red) and prompt (pink) which gave a lifetime of 6.9 and 0.38 ns for **1** and TPTA respectively.

References

1 A. Yadav, M. S. Deshmukh and R. Boomishankar, *J. Chem. Sci.*, 2017, **129**, 1093-1103.

2 G. M. Sheldrick, *Acta Crystallogr. A: Foundations of Crystallography* 2008, **64**, 112-122.

3 S. Kurtz, T. Perry, *J. Appl. Phys.* 1968, **39**, 3798-3813.

4 M. Frisch, G.Trucks, H. Schlegel, *GAUSSIAN 03, Revision B. 05, Gaussian, Inc., Wallingford, CT*, 2004.

5 A. K. Gupta, A. Steiner and R. Boomishankar, *Dalton Trans.* 2012, **41**, 9753–9759.

6 Z. Guo, R. Cao, X. Wang, H. Li, W. Yuan, G. Wang, H. Wu and J. Li, *J. Am. Chem. Soc.* 2009, **131**, 6894-6895.

7 W.-J. Xu, P.-F. Li, Y.-Y. Tang, W.-X. Zhang, R.-G. Xiong and X.-M. Chen, *J. Am. Chem. Soc.* 2017, **139**, 6369−6375

8 M. Mon, J. Ferrando-Soria, M. Verdaguer, C. Train, C. Paillard, B. Dkhil, C. Versace, R. Bruno, D. Armentano and E. Pardo, *J. Am. Chem. Soc.* 2017, **139**, 8098-8101.

9 M. Guo, H.-L. Cai and R.-G. Xiong, *Inorg. Chem. Commun.* 2010, **13**, 1590-1598.

10 A. K. Srivastava, B. Praveenkumar, I. K. Mahawar, P. Divya, S. Shalini and R. Boomishankar, *Chem. Mater.*, 2014, **26**, 3811-3817.

11 A. K. Srivastava, P. Divya, B. Praveenkumar and R. Boomishankar, *Chem. Mater.*, 2015, **27**, 5222-5229.

12 A. K. Srivastava, T. Vijayakanth, P. Divya, B. Praveenkumar, A. Steiner and R. Boomishankar, *J. Mater. Chem. C*, 2017, **5**, 7352-7359.